GMPLS/PCE-controlled Multi-Flow Optical Transponders in Elastic Optical Networks [Invited]

Ricardo Martínez, Ramon Casellas, Ricard Vilalta and Raül Muñoz

***Abstract*—Elastic Optical Networks (EONs) aim at considerably improving the network spectrum efficiency (by means of a flexible grid) compared to the traditional optical transport networks operating with fixed frequency spacing. In such flexible networks, connections are accommodated into the so-called "frequency slots" which are dynamically established depending on client data rates and selected signal modulation formats. Key enablers to develop such network infrastructure are the bandwidth variable optical cross-connects (BV-OXCs) and the BV transponders. For the latter, a Multi-flow Optical Transponder (MF-OTP) is being considered as an appealing solution due to its support for high-rate super-channels as well as its *elasticity* where optical connections can be reconfigured flexibly according to the required traffic requests.**

The dynamic selection (path computation) and automatic network configuration of both optical spectrum and MF-OTPs resources are handled by a control plane entity. Herein a distributed Generalized Multi-Protocol Label Switching (GMPLS) control plane combined with an active Path Computation Element (PCE) are adopted for the dynamic instantiation of flexgrid optical connections. To fully control the MF-OTP attributes and capabilities, specific extensions are required to both GMPLS routing and signaling. We propose and experimentally validate such extensions considering two information models, namely: *partial* and *full*. The difference between both models lies on the information related to optical spectrum status (carried by *full*) on the MF-OTP interfaces attached to the BV-OXCs. Furthermore a novel online Routing, Spectrum and Modulation Assignment (RSMA) algorithm is conceived. The RSMA adopts both models to compute paths trying to optimize the spectral link and MF-OTP resources when dynamically serving flexgrid connections. The experimental evaluation compares, for both models, the attained RSMA performance with respect to the blocking probability as well as the setup and path computation delays.

***Index Terms*—Multi-Flow Optical Transponders (MF-OTPs), Generalized Multi-Protocol Label Switching (GMPLS), Path Computation Element (PCE).**

I. Introduction

The increase of the generated data traffic within the backbone infrastructure (estimation of 35% per year [1]), due to the emergence of more dynamic and bandwidth-consuming services (e.g., mobile Internet, high-definition video, cloud-based applications), is forcing operators to seek for solutions addressing such challenges in a cost-efficient way. In this regard, an appealing solution relies on exploiting as much as possible the optical spectrum provided by the installed optical fibers [2]. This solution is referred to as flexgrid or elastic optical networks (EONs).

The goal of EONs is to provide finer granularity than current fixed ITU-T DWDM grid (typically using 50 GHz of channel spacing) attaining a more efficient and flexible use of the optical spectrum. In particular, EONs partition the optical spectrum into a grid with a finer channel spacing such as 6.25 GHz or 12.5 GHz [3]. By doing so, optical connections (Label Switched Paths, LSPs) with different bit-rate demands are adaptively and flexibly accommodated (according to the path distance and modulation formats) into variable sized frequency slots (FS) allocating as much as optical spectrum as required. Each FS is defined by its nominal central frequency (NCF, parameter n) and its slot width (parameter m) [4]. Thus, the FS for a given LSP is completely determined by n which specifies the central frequency with respect to an anchor frequency (193.1 THz + n*0.00625 THz) and m determining the total slot width (m*12.5 GHz). NCFs are defined following a specific channel spacing grid (e.g., 6.25 GHz) where every FS results as a multiple of fixed slot widths (i.e., multiples of 12.5 GHz).

The key elements for deploying EONs are two [2], namely the bandwidth-variable transponders (BVTs) and the bandwidth-variable optical cross-connects (BV-OXCs). BVTs generate optical signals supporting multiple modulation formats and bit-rates that can be dynamically adapted according to the clients signal needs and network conditions [5]. Such a flexibility allows the operator optimizing network capacity to attain the most efficient use of the optical spectrum. In this regard, two strategies are applied: *distance-adaptive* [6] or *rate-adaptive*. In the former, for a given bit-rate and path distance the selected feasible modulation format is the one requiring the minimum spectral resources (i.e., slot width). In the latter, the minimum spectrum resources allocated for a flexgrid LSP can be dynamically varied (using the same modulation format) according to the client traffic demands (i.e., *elasticity)*. This states the trade-off between distance/bit-rate and required optical spectrum. BV-OXCs, on the other hand, allow switching an optical signal based on the FS (i.e., central frequency and spectrum width) rather than on a fixed wavelength.

To increase further the flexibility and reconfigurability in EONs, BVTs are being designed to support generating multiple FSs. These FSs can be flexibly associated to client layer demands (e.g., IP). These are routed in an aggregated way (forming *super-channels*) or independently towards different destinations by means of the switches and filters within the BV-OXCs. Herein the term of super-channel is considered as the contiguous logical aggregation of different generated FSs. Those BVTs capable of generating a number of FSs are referred to as *multi-flow optical transponder* (MF-OTP) or sliceable bandwidth variable transponder (SBVT) [1], [7].

In this work, we extend our previous work in [8] focusing on the automatic control and management of MF-OTPs when dynamically setting up flexgrid LSPs with different bit-rate demands. We rely on using both a distributed GMPLS control plane (routing and signaling) for the automatic provisioning/tear-down of LSPs and a centralized path computation provided by the Path Computation Element (PCE) [9].

The above objective is addressed from a twofold perspec-

Manuscript received June 1, 2015.

R. Martínez, R. Casellas, R. Vilalta and R. Muñoz are with CTTC, Spain (e-mail: ricardo.martinez@cttc.es).

tive: i) specifying the GMPLS protocol extensions to support the discovery and control of MF-OTPs; ii) a novel online RSMA algorithm to compute the path and network resources (FS and MF-OTPs) for every new LSP demand [9], [10]. The proposed GMPLS extensions enhance both the routing and signaling protocols. For the routing protocol (GMPLS OSPF-TE), three different information models namely, *no information*, *partial* and *full* can be adopted. Each model encompasses different levels for disseminating MF-OTPs Traffic Engineering (TE) attributes and capabilities: ranging from *no information* up to to the most detailed information (at NCF granularity) used by *full* model. For the signaling protocol (GMPLS RSVP-TE), an extension to explicitly allocate the computed MF-OTP resources at both ingress and egress nodes is designed. Such extensions pave the way for devising a RSMA algorithm that dynamically computes flexgrid LSPs between two remote MF-OTPs. The aim of the algorithm is to serve LSP demands trying to achieve the most efficient use of the network resources. The RSMA relies on a distance-adaptive mechanism which upon receiving a flexgrid LSP request, computes the spatial path (i.e., nodes and links), the FS and the modulation format to be configured at the MF-OTP endpoints.

The proposed GMPLS extensions and devised RSMA algorithm are experimentally validated and evaluated upon dynamic traffic conditions. The results are obtained at the control plane level within the ADRENALINE testbed, aiming at comparing the attained performance (in terms of connection blocking probability) when either *partial* or *full* routing information models are applied.

The rest of this paper is organized as follows: in Section II we overview the related work and the considered MF-OTP architecture. In Section III, we present an example of the RSMA computation with respect to the used MF-OTP information model (i.e., *partial* or *full*). Section IV describes required GMPLS protocol extensions along with the devised RSMA algorithm. The experimental performance evaluation of the RSMA algorithm using *partial* and *full* MF-OTPs models is presented in Section V. Finally, in Section VI we conclude the paper.

II. Related Work and Considered MF-OTP Architecture

MF-OTPs support the capability to identify client data traffic (at sub-wavelength granularity) that arrives from a single client interface (e.g., a router) using, for instance, packet headers, and map them into multiple connections with different FS, data rates and optical reaches [7]. This allows MF-OTP supporting point-to-multipoint connections where individual optical connections are routed towards different destination nodes. Another interesting feature of MF-OTPs is the capability of creating super-channels LSPs. Super-channels connections are made up of two or more contiguous optical spectrum aggregated FSs. Each FS of is generated by individual *sub-transceivers* (also referred to as *sub-carriers*) equipped into the MF-OTP. Super-channel connections are transported through the BV-OXCs and detected as a single entity (i.e., no guard bands between the different FSs are needed).

Different MF-OTP implementations supporting a number of transmission techniques have been proposed in the literature. In [1] it is reported three of the most promising transmission techniques to build a MF-OTP, namely: Nyquist wavelength-division multiplexing (NWDM), orthogonal frequency-division multiplexing (OFDM), and time frequency packing (TFP). The capabilities of these techniques are compared along with discussing practical issues around manufacturing, integration and programmability.

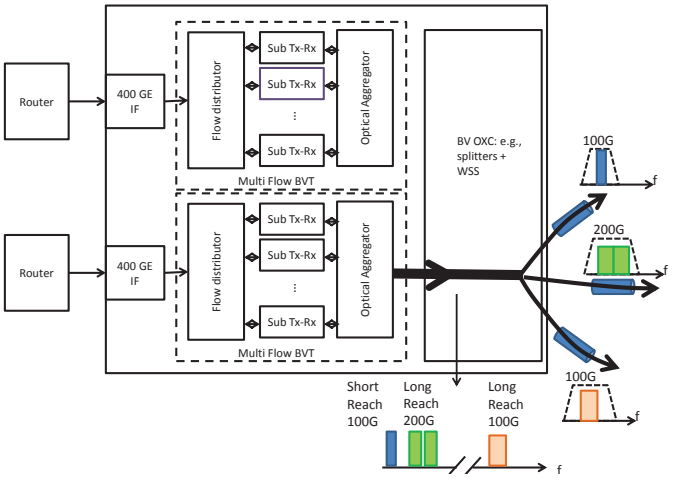

Fig. 1. Flexgrid Edge Node: MF-OTP and BV-OXC

Figure 1 depicts the architecture of a flexgrid edge node integrating a pool (1 or more) of MF-OTP devices connected to a BV-OXC. Focusing on the MF-OTP, we adopt the architecture described in [7]: a MF OTP is formed by flow distributor, a set of laser sources (sub-transponders) and an optical aggregator. The flow distributor enables identifying which client traffic will be transmitted into a single sub-transponder within the optical layer. In this regard, the bit rate and bandwidth for each sub-transponder are tuned by modifying the modulation format, baud rate, coding, etc. This enables adapting the optical flexgrid LSP to the distance of the traversed path as well as the physical network conditions (e.g., impairments). Finally, all generated sub-carriers are multiplexed over a single line interface connected to the BV-OXC. In Fig. 1, four sub-carriers are used generating: one optical connection for a short reach path operating at 100 Gb/s, a super-channel formed by two FSs transporting 200 Gb/s for a long reach connection, and a 100 Gb/s long reach LSP made up of a single FS.

Alternatively to the above MF-OTP implementation using N lasers to generate N sub-carriers, in [11] it is proposed a more cost-efficient solution based on multiwavelength source. The multiwavelength source is capable of generating N sub-carriers by using a single laser. In this work, however, the first MF-OTP approach is adopted (i.e., 1 sub-transponder per each FS).

Although the automatic control of flexgrid networks (in terms of FS allocation between BV-OXC links) have received significant attention in the literature during the last years [10], [12], the explicit control and configuration of MF-OTPs have not been studied thoroughly. In this regard, in [13], it was demonstrated the configuration of SBVTs using a Software Defined Network (SDN) control where extensions to the OpenFlow protocol were proposed and validated to configure the SBVTs (i.e., FS, modulation format, etc.). In [8], on the other hand, we presented novel GMPLS routing and signaling extensions to automatically control and configure MF-OTPs when dynamically accommodating flexgrid LSPs.

Herein we rely on the main outcomes achieved in [8], but providing a more detailed description of the proposed RSMA algorithms along with further and more exhaustive performance evaluation of the whole system. Last but not least, it is worth mentioning that the proposed RSMA algorithms in this work enhance the one presented by the authors in [12]. Such an improvement stems from the fact that the capabilities and restrictions imposed by the MF-OTPs are taken into account when computing and setting up end-to-end flexgrid LSPs.

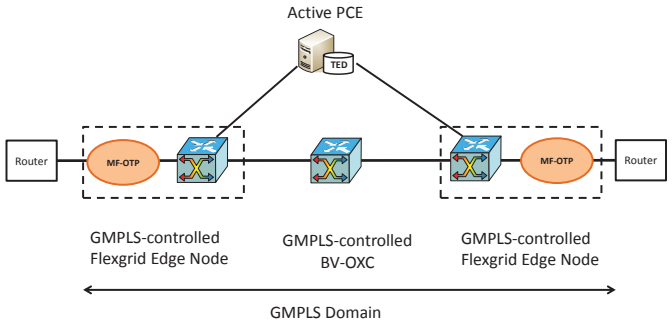

Fig. 2. GMPLS/PCE controlled EON

In Fig. 2 it is represented the considered GMPLS/PCE-controlled EON infrastructure. In such a network, the active PCE computes and instantiates the establishment of flexgrid LSPs between a pair of flexgrid edge nodes. A path may traverse one or more BV-OXCs between the LSP endpoints. Every network node (i.e., flexgrid edge and BV-OXCs) is controlled and configured by a GMPLS control plane instance. The control plane automatically allocates and occupies the computed FS and MF-OTP resources to set up the flexgrid LSP. For the sake of clarification, we consider that the GMPLS routing domain does not comprise the client nodes (i.e., router). In other words, the routing information is restricted to flood the topology and TE link and node attributes of both flexgrid edge and BV-OXCs nodes.

III. Problem Statement: RSMA Computation with MF OTP

Each flexgrid LSP request (req) specifies the endpoints (source s and destination d nodes) and bit-rate (R in Gb/s). An active PCE computes the path and initiates the establishment of req. The RSMA algorithm is executed in the PCE [9], [10]. If the path computation succeeds, the PCE sends a PCE protocol (PCEP) message named PCInitiate to node s (ingress) to start the establishment of the new LSP [14]. The PCInitate message specifies the Explicit Route Object (ERO) including the spatial path and the spectral resources (FS). Furthermore, the PCInitiate message also carries MF-OTP specific information to be configured at the LSP endpoints: selected sub-carriers (using local identifiers - IDs - within the MF-OTP), the employed modulation format, the FS (i.e., n and m) per sub-carrier, etc. Consequently, the RSMA needs details of the MF-OTP attributes and capabilities to perform such path computation.

The TE and resource information of MF-OTPs are flooded by the routing protocol and gathered at the PCE's Traffic Engineering Database (TED). The contents are used as the input information for the RSMA algorithm executed at the PCE. In the *no information* model, the RSMA only operates with the topology and network link attributes between BV-OXCs. The selection and configuration of MF-OTP resources is locally done at the corresponding endpoint (i.e., s and d) by the signaling mechanism. In the *partial* model, the PCE's TED collects limited details of the MF-OTP interfaces, namely the number of available sub-transponders. Finally, in the *full* model, the partial view of MF-OTPs is extended with aggregated optical spectrum utilization (for both transmission - Tx - and reception - Rx - directions) over the MF-OTP and BV-OXC interface. This would facilitate the RSMA algorithm selecting a feasible FS avoiding overlapping with the optical spectrum occupied by other optical LSPs. In the following, we exclusively focus on the *partial* and the *full* routing information models.

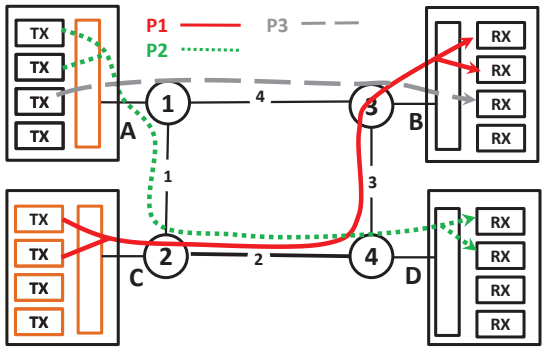

Fig. 3. Example of 3 (P1, P2 and P3) flexgrid LSPs using MF-OTPs.

For a request req the RSMA algorithm computes the (shortest) path ensuring sufficient continuous and contiguous unused optical spectrum through the entire path. The FS is selected from a set of feasible solutions using the first-fit algorithm. In the example shown in Fig. 3, three LSPs (P1, P2 and P3) are sequentially established. P1 is a super-channel (formed by two FSs) using two sub-carriers (at both MF-OTP C and D) and is set up through the path 2C-4-3B occupying the logically aggregated FS formed by NCFs 1-4. Next, P2 is set up between 1A and 4D. Regardless of the MF-OTP information model, P2 is provisioned as a super-channel connection (formed by 2 FSs requiring 2 sub-carriers) along the path 1A-2-4D and allocates the FSs using the NCFs between 5 and 8. Observe that P2 is set up over an available FS without incurring on optical spectrum collision with the established P1. Finally, P3 must be set up from MF-OTP labeled by 1A to 3B. Using MF-OTP *partial* model (i.e., no available NCF information of MF-OTP interfaces is flooded), P3 is computed through the path 1A-3B trying to allocate the FS composed by NCFs 1-2. Nevertheless, although such an FS is available on the link 4 (i.e., between nodes 1 and 3), P3 would fail as shown in Fig. 4.a since that FS is already being used by P1. This example allows realizing that *partial* model does complicate the spectrum allocation (FS computation) in MF-OTP interfaces. The *full* model allows mitigating such problems providing to the RSMA algorithm the NCF status on the links connecting the MF-OTPs with their respective BV-OXCs (see Fig. 4.b). Therefore, in the *full* model, the RSMA algorithm computes P3 through the route 1A-3B but selecting the FS formed by the unused 9 and 10 NCFs which leads to avoid the spectrum collision with established LSPs.

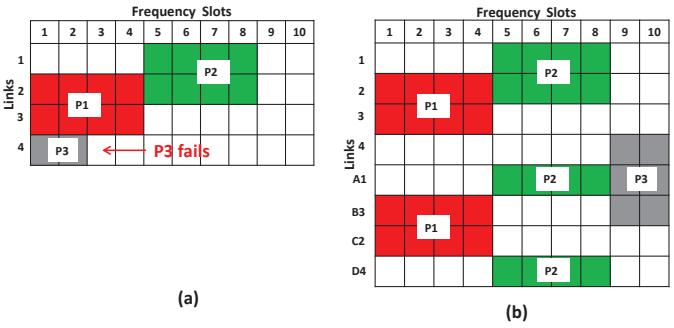

Fig. 4. Resulting spectrum allocation using either a) *partial* or b) *Full* MF-OTP information models.

IV. GMPLS Protocol Extensions and Proposed RSMA Algorithm

This section details the required GMPLS routing and signaling extensions in support for controlling MF-OTPs along with the description of the devised RSMA applicable to both *partial* and *full* models.

A. Routing and Signaling Protocol Extensions

The strict control of MF-OTPs within the context of GMPLS control plane requires specific extensions in both routing and signaling protocols. For both *partial* and *full* information models, the OSPF-TE protocol floods the MF-OTP TE attributes and capabilities using the Port Label Restriction (PLR) sub-Type-Length-Value (TLV). We extend the PLR sub-TLV, which is included into the top Link TLV of GMPLS OSPF-TE [15], as proposed in [16]. In Fig. 5(a) it is shown an OSPF-TE Link State Update carrying the PLR sub-TLV for the *full* information model. The PLR (Type 26) carries for each individual MF-OTP:

- *TxSubTrnsp* specifying the number of sub-transceivers (sub-carriers) for Tx direction.
- *RxSubTrnsp* specifying the number of sub-transceivers (sub-carriers) for Rx direction.
- *AvailTxTrnsp* specifying the number of available (not used) sub-transceivers (sub-carriers) for the Tx direction.
- *AvailRxTrnsp* specifying the number of available (not used) sub-transceivers (sub-carriers) for the Rx direction.
- Aggregated NCF status per direction (Tx and Rx) on the interface between the MF-OTP and the BV-OXC. To this end, the Label TLV (Type set to 1) [17] uses a bitmap coding, where every supported NCF is represented by a bit: 1 available and 0 occupied. The bitmap coding for each NCFs is referenced with respect to the *lowest* NCF (contained in the Label TLV). The lowest NCF has the lowest n. Herein, lowest n is 0, thus the lowest NCF is the anchor frequency (i.e., 193.1 THz).

Once the route for a LSP request req is computed, the path is passed as an ERO to be carried into the RSVP-TE Path message to set up the LSP. The ERO contents specify the spatial path (i.e., node and link identifiers to be traversed by the LSP), the FS to be allocated and specific configuration characteristics for the MF-OTPs at s and d. The latter requires extending the RSVP-TE ERO sub-objects to support the so-called Explicit Transponder Control (ETC) sub-object (Type 10). The proposed ETC is formed by a variable list of Transponder TLVs. This allows the configuration of a set of sub-carriers generating the FSs forming a super-channel LSP. Each Transponder TLV (Type 1) contains 4 sub-TLVs:

- *Sub-Transponder Id* (Type 5005) locally identifies a sub-transponder within the MF-OTP.
- *Sub-Carrier FS* (Type 5006) specifies the FS (n and m) to be allocated by the respective sub-transponder / sub-carrier.
- *Modulation Format* (Type 5001) configures the sub-transponder to use a concrete modulation format (e.g., DP-QPSK, DP-8QAM or DP-16QAM).
- *Forwarding Error Correction* (FEC, Type 5002) allows configuring the FEC.

Fig. 5(b) depicts a captured RSVP-TE Path message carrying the ERO information: unnumbered interface ID (node and link ID), the label sub-object (specifying the allocated FS) and the proposed ETC extension.

B. MF OTP RSMA Algorithm

The RSMA algorithm relies on an iterative Constrained Shortest Path First (CSPF) mechanism wherein for each demand req the shortest path (SP) with respect to the link cost is computed to achieve the most efficient use of both optical spectrum and MF-OTP resources. The algorithm output is the ERO formed by the spatial path, the selected FS and the sub-transponders attributes (i.e., FS and modulation format). To do this, the algorithm enhanced the a previous one proposed by the authors in [9] operating iteratively starting from the most efficient modulation format until a feasible solution is found considering the sub-transponder capabilities at the endpoints. If all modulation formats are checked and no solution is found, req is blocked.

The following notation is defined to describe the RSMA algorithm whose pseudo-code is as well provided.

req	Flexgrid LSP request.
s, d	The source and destination nodes for req.
E	The set of network links.
V	The set of network nodes.
$d[i]$	The path cost (in km) from s to node i.
$p[i]$	The predecessor node to reach i.
$NCF[i]$	The set of available and common NCFs at i constructed from s.
S	The set of nodes already considered in the shortest path.
Q	The set of candidate nodes sorted by the shortest cost from s, not considered yet in S.
R	Requested bit-rate in Gb/s by req.
MF	Set of supported modulation formats ordered by their spectral efficiency.
F_n	Set of MF-OTPs at node n.
$T_{f,n}$	Set of available sub-carriers (*AvailTxTrnsp*) for Tx at MF-OTP $f \in F_n$.
$\|T_{f,n}\|$	Number of available sub-carriers for Tx at MF-OTP $f \in F_n$.
$R_{f,n}$	Set of available sub-carriers (*AvailRxTrnsp*) for Rx at MF-OTP $f \in F_n$.
$\|R_{f,n}\|$	Number of available sub-carriers for Rx at MF-OTP $f \in F_n$.
$UT_{f,n}$	Set of used sub-carriers per req for Tx at MF-OTP $f \in F_n$.

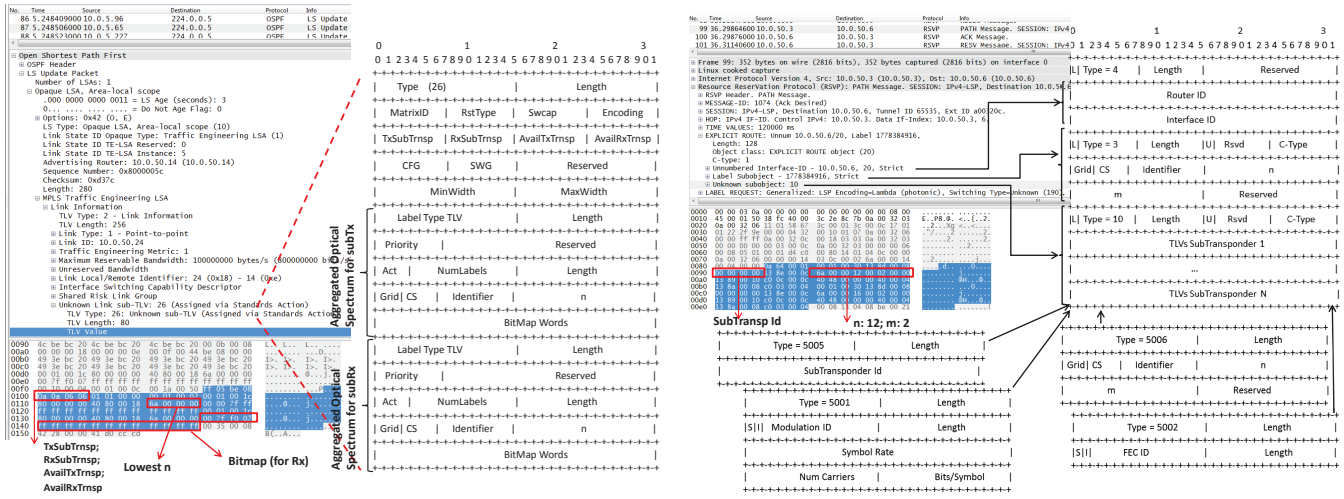

(a) OSPF-TE PLR sub-TLV extension in support of MF-OTP. (b) RSVP-TE ERO ETC sub-object extension in support of MF-OTP.

Fig. 5. Implemented OSPF-TE and RSVP-TE extensions in support of MF-OTP.

$UR_{f,n}$	Set of used sub-carriers per req for Rx at MF-OTP $f \in F_n$.
n_{sc}	Number of required sub-carriers at both s and d by req according to $mf \in MF$.
B	Fixed optical spectrum (in GHz) occupied by a sub-carrier $tx \in T_{f,n}$ or $rx \in R_{f,n}$.
SW	Optical spectrum (in GHz) required by req according to $mf \in MF$; $SW = B * n_{sc}$.
$MaxD_{mf}$	Maximum distance (in km) supported by $mf \in MF$.
P	Shortest path between s and d satisfying spectrum continuity and contiguity constraints for SW not exceeding $MaxD_{mf}$.
$setNCF_{f,n}$	Set of unused NCFs at link between MF-OTP $f \in F_n$ and BV-OXC n.
NCF_l	Unused NCFs at link $l \in E$ (i.e. pair of BV-OXCs).
l_{cost}	Link cost (in km) of $l \in E$.
$getnode(Q)$	Returns the first node stored in the Q set.
$checkSCgC$	For $v \in V$ and SW, returns $TRUE$ if SW available and spectrally contiguous NCFs exist in $NCF[v]$; $FALSE$ otherwise.

For a given modulation format (mf), it is checked whether the requested bit rate (R) is supported by mf (see Algorithm 1). We consider that each MF-OTP has N sub-transponders / sub-carriers operating at a fixed baud rate (e.g., 25 Gbaud/s). This entails that the optical spectrum occupied by each sub-carrier, regardless of the modulation format, is as well fixed (B). Therefore, if R is not multiple of the transport capacity of a sub-carrier at mf (i.e., using one or more sub-carriers), then mf is discarded. Otherwise, the number of required sub-carriers (n_{sc}) is computed. Next, at s and d nodes, it is verified whether the computed n_{sc} sub-carriers are available for both Tx and RX, respectively. If not, mf is discarded. After that, the FS width (i.e., SW) is computed to accommodate req using n_{sc} at mf; SW is obtained multiplying the individual FS width of each sub-carrier (i.e., $m = 2$ corresponding to 25 GHz using a channel spacing of 6.25 GHz) by the computed n_{sc} sub-carriers. Next, a modified Dijkstra algorithm (P function) computes the shortest path between s and d ensuring both the spectrum continuity (SCC) and the spectrum contiguity constraints (SCgC) for SW. The SCC is ensured by the RSMA selecting the same (unused) SW optical spectral resources (i.e., NCFs) for req on every link traversed by the path; on the other hand, SCgC is ensured forcing that those selected NCFs are spectrally contiguous [18]. The P function dealing with the modified Dijkstra algorithm is detailed in Algorithm 2. If such an algorithm does not succeed (e.g., failing either SCC or SCgC) or the maximum supported distance by mf (i.e., $MaxD_{mf}$) is exceeded, then mf is discarded. Otherwise the computed route (ERO) is returned to s to start the LSP establishment. The selected FS for req from the computed NCFs through the entire path satisfying the aforementioned set of constraints is chosen adopting the first-fit algorithm.

P function starts with the $init$ process (Algorithm 3). For all network nodes ($u \in V$) different than s, the path cost (i.e., $d[u]$) is set to infinity. The NCF set at each node (i.e., $NCF[u]$) is pre-loaded to all the supported NCFs in the whole network. Nevertheless, if the *full* information model is applied, observe that $NCF[s]$ is pre-set to the resulting intersection of the unused NCFs in both source and destination MF-OTP - BV-OXC links. Such a $NCF[s]$ computation is not required when adopting the *partial* model as discussed in Section 3.

In the main loop of P, if either d node is reached or the candidate Q set becomes empty, Algorithm 2 stops. In the latter, the response informs that the modified Dijkstra algorithm did not succeed to find a feasible path satisfying the constraints.

The $Qset$ (Algorithm 4) updates the candidate nodes in the Q set. For each outgoing link (i.e., l) connecting current node v to node w, it checks whether the available NCFs on link l (i.e., NCF_l) intersecting with the accumulated unused NCFs from node s to node v (i.e., $NCF[v]$) is not empty. The resulting intersection is stored in $NCF[w]$. If this set of NCF at node w is empty, then no common and available NCFs from s to w exist, thus link l is discarded. This allows ensuring the SCC restriction. Next the SCgC restriction is ensured by means of the $checkSCgC$ function. The aim of $checkSCgC$ is to verify that SW contiguous and available NCFs are available into $NCF[w]$ to accommodate the req. If such verification fails, the link l is discarded.

Algorithm 1 On-line RSMA for $req(R, s, d)$

for all $mf \in MF$ **do**
  if R NOT supported by mf **then**
    Continue
  end if
  Compute n_{sc} ▷ for R using mf
  for $fi \in F_s$ **do** ▷ MF-OTPs at s
    if $|T_{fi,s}| < n_{sc}$ **then**
      $UT_{fi,s} = NULL$
    else
      Compute $UT_{fi,s}$ ▷ select n_{sc} for Tx of fi at s
      Break
    end if
  end for
  for $fe \in F_d$ **do** ▷ MF-OTPs at d
    if $|R_{fe,d}| < n_{sc}$ **then**
      $UR_{fe,d} = NULL$
    else
      Compute $UR_{fe,d}$ ▷ select n_{sc} for Rx of fe at d
      Break
    end if
  end for
  if $UT_{fi,s} == NULL$ OR $UR_{fe,d} == NULL$ **then**
    Continue
  else
    Compute SW
    Compute $setNCF_{fi,s}$ ▷ *full* model
    Compute $setNCF_{fe,d}$ ▷ *full* model
    if $P == FALSE$ **then** ▷ no feasible path
      Continue
    else
      Generate ERO for req
    end if
  end if
end for

Algorithm 2 Modified Dijkstra algorithm (P function)

Input: s, d, SW, $MaxD_{mf}$
Input: $setNCF_{fi,s}$, $setNCF_{fe,d}$ ▷ *full* model
$init$
$v \leftarrow s$
while 1 **do**
  $Qset$
  if $Q := \emptyset$ **then**
    return $FALSE$
  else
    $v = getnode(Q)$
  end if
  if $v == d$ **then**
    return $TRUE$
  else
    $Q := Q - v$; $S := S \cup v$
  end if
end while

Once both SCC and SCgC constraints are ensured, the path cost to node w is obtained using the link cost (i.e., l_{cost}). It is checked that the total cost to w (i.e., $d[w]$) does not exceed the maximum permitted distance by the targeted modulation format (i.e., $MaxD_{mf}$). If this occurs link l is discarded. Alternatively, the computed path to node w is considered as feasible. If no previous path to w exists, then w is added to the Q set. Otherwise, two routes to w are feasible. In such a situation, the algorithm applies the criteria to select the one with the shortest path cost. This may require to execute $relax\_link$ function (Algorithm 5) for updating a previous computed path to w.

Algorithm 3 Initialization $init$

Input: s, d
Input: $setNCF_{fi,s}, setNCF_{fe,d}$ ▷ *full* model
for all $u \in V$; $u \neq s$ **do**
  $d[u] = \infty$
  $p[u] = u$
  $NCF[u] = all$
end for
$S := \emptyset$; $Q := \emptyset$
$d[s] = 0$
$p[s] = \emptyset$
$NCF[s] = setNCF_{fi,s} \cap setNCF_{fe,d}$ ▷ *full* model
$NCF[s] = all$ ▷ *partial* model
$S := S \cup s$

Algorithm 4 Update candidate list $Qset$

Input: $v, Q, S, SW, MaxD_{mf}$
for all $l = v \rightarrow w$; $l \in E$ **do**
  if $S \cap w \neq \emptyset$ **then**
    Continue
  end if
  $NCF[w] = NCF[v] \cap NCF_l$
  if $NCF[w] == \emptyset$ **then** ▷ SCC failure
    Continue
  end if
  if $checkSCgC(w, SW)$ == FALSE **then** ▷ SCgC failure
    Continue
  end if
  $d[w] = d[v] + l_{cost}$
  if $d[w] > MaxD_{mf}$ **then** ▷ Max. distance per mf exceeded
    Continue
  end if
  if $Q \bigcap w = \emptyset$ **then**
    $Q := Q + w$
  else ▷ $\hat{w}$ previous path to w in Q
    if $d[\hat{w}] < d[w]$ **then**
      Continue
    else if $d[\hat{w}] \geq d[w]$ **then**
      $relax\_link(\hat{w}, w, v)$
    end if
  end if
end for

As mentioned the RSMA algorithm is applied for both *partial* and *full* models. However, it is worth stressing that in the *full* model the aggregated optical spectrum availability

Algorithm 5 Relax link

Input: $\hat{w}, w, v$
$d[\hat{w}] = d[w]$
$p[w] = v$
$NCF[\hat{w}] = NCF[w]$

on the MF-OTP interfaces at s and d is added to ensure both the SCC and SCgC for the computed SW GHz.

V. Experimental Performance Evaluation

In this section, the performance evaluation of the proposed on-line RSMA algorithm when *partial* and *full* MF-OTPs models are used is conducted. The numerical results are obtained at the GMPLS control plane of the ADRENALINE testbed [14], [19] where flexgrid optical hardware (i.e., MF-OTPs and BV-OXCs) is emulated. The GMPLS control plane of ADRENALINE testbed is an experimental platform providing full and real implementation of the involved processes and control protocols (routing and signaling) as well as the active PCE. In this work the implemented GMPLS control plane is enhanced with the routing and signaling extensions described in section IV-A. Every network node has a physical GMPLS control plane instance enabling the control communication with other nodes using a dedicated data communication (control plane) network. Nevertheless control plane decisions when setting up a flexgrid LSP do not result on a real configuration of underlying optical hardware since ADRENALINE testbed lacks of such optical infrastructure. This is the reason why we state that the optical hardware is emulated.

Two figures of merit are used for the performance evaluation: the connection blocking probability (BP) and the delay (in ms) for both the connection setup and the RSMA computation. In particular, BP allows indicating the efficiency of the RSMA algorithm when operating with either *partial* or *full* model at the time of handling the network resources when dynamically setting up flexgrid LSPs.

A. Network Topology and Experimental Details

The network topology follows a Spanish EON formed by 22 links and 14 BV-OXCs (see Fig. 6). Each optical link has its own distance (in km) and supports 128 NCFs ($n : 0..127$) with a channel spacing of 6.25 GHz. As the control links (used for exchanging routing and signaling messages) are considered in fiber, link propagation delays are as well taken into account to deliver control messages. This is used for computing the setup delay for establishing LSPs. Every network node is controlled by a GMPLS control plane implemented on a Linux-based router with an Intel Xeon 3 GHz processor. The active PCE is co-located with N1. As depicted in Fig. 6, 11 nodes are equipped with MF-OTPs. Such a pool of nodes constitutes the possible pair of source and destination nodes for any req. The rest of nodes (a total 3) are intermediate optical switches. The number of sub-carriers equipped in each MF-OTP is varied: 5, 10, 15 and 20. The supported modulation formats by the sub-carriers are: DP-QPSK, DP-8QAM and DP-16QAM.

Table I depicts for each of the supported modulation formats (mf) the bits/symbol, the Gb/s (assuming a fixed symbol rate of 25 Gbauds/s) and the maximum supported path distance (i.e., $MaxD_{mf}$). The requested bandwidth (R) for each req is uniformly distributed as multiples of 100 Gb/s up to 500 Gb/s. In Table I, it is also shown the number of required sub-carriers for each possible R bit rate.

TABLE I
Number of sub-carriers & $MaxD_{mf}$ per mf and bit rate (R)

mf	DP-QPSK	DP-8QAM	DP-16QAM
bits/symbol	4	6	8
bi rate (Gb/s)	100	150	200
$MaxD_{mf}$ (km)	3000	1000	650
R (Gb/s)	n_{sc}		
100	1	-	-
200	2	-	1
300	3	2	-
400	4	-	2
500	5	-	-

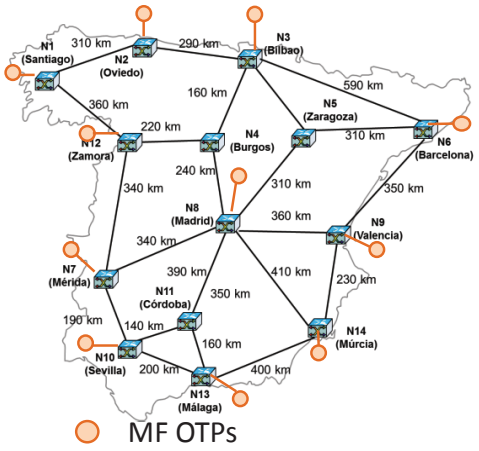

Fig. 6. Transport network topology with MF-OTPs.

We assume uniform traffic between all the nodes equipped with MF-OTPs. The arrival process of the LSP demands is Poisson with a mean inter-arrival time of 10s. The holding time (HT) of the LSPs is exponentially modeled whose mean is varied to obtain different network loads.

Each sub-carrier has a fixed FS width of $m = 2$ (i.e., 25 GHz). Thus, a 400 Gb/s LSP using 2 sub-carriers at DP-16QAM uses a FS width of 50 GHz whilst the same LSP using 4 sub-carriers with DP-QPSK requires a FS of 100 GHz.

B. Experimental Results and Analysis

Table II gathers the obtained numerical results varying the HT (i.e., 25, 50, 75 and 100 s) when the RSMA algorithm adopts either *partial* or *full* models. These results are presented as: the time required by the RSMA algorithm to be executed; the average setup time (computed as the elapsed time between the LSP request is received and when the LSP is actually set up); the RSMA errors (i.e., path computation failures); the signaling errors; and the BP.

In general for all HT values, the use of *full* model does lower the BP compared to the *partial* model. This is attained at the expenses of slightly increasing the complexity of the RSMA algorithm along with the generated control plane overhead (MF-OTP spectrum status information). LSP failures are divided into: path computation (i.e., RSMA failures) and signaling errors. In both models, we observe that RSMA errors are mainly caused by the lack of available sub-carriers

TABLE II
EXPERIMENTAL DELAY AND BP RESULTS

		Delay (ms)		Error		
HT (s)	Model	RSMA	Setup	RSMA	Sign.	BP (%)
25	Partial	11.2	51.4	1	225	22.6
	Full	12.3	50.9	6	12	1.8
50	Partial	11.5	51.8	9	278	28.7
	Full	11.3	50.9	24	3	2.7
75	Partial	10.7	51.7	23	322	34.5
	Full	10.9	50.4	34	18	5.2
100	Partial	10.5	50.9	26	331	35.7
	Full	11.4	50.8	60	8	6.8

at the time of computing the route. That is, no sufficient sub-carriers are available at either s or d for req. On the other hand, signaling errors occur when the computed LSPs are being actually set up. The main difference between both (*partial* and *full*) models lies on the signaling errors. In the *partial* model, these errors principally happen due to the difficulties to deal with either SCC and SCgC. Thus, contention on the MF-OTP interfaces with existing LSP is likely to occur. Applying the *full* model, these problems are lowered. Indeed, the RSMA algorithm is aware of the optical spectrum status of MF-OTP interfaces which in turn facilitates dealing with the required end-to-end spectrum restrictions (SCC and SCgC). Signaling errors appearing in the *full* model could be due to either concurrent LSPs being signaled or the RSMA algorithm operates with outdated PCE's TED. We can observe that the differences with respect to the setup and RSMA delays are negligible, since both models use (practically) the same RSMA algorithm.

Figure 7 depicts the BP when the number of sub-carriers per MF-OTP is varied (i.e., 5, 10, 15 and 20) and the HT is fixed to 100s. We can observe that as the number of sub-carriers is increased the BP attained by *full* model is enhanced since the lack of sub-carriers is less troublesome for the RSMA computation. In the *partial* model, the increase of the number of sub-carriers also allows improving the BP but up to a certain value (10 sub-carriers). Above this value, the achieved improvement is negligible since the errors are not due to the lack of available sub-carriers during the path computation but the spectrum restriction problems that the signaling encounters. Consequently, regardless of increasing the number ensuring both SCC and SCgC when the *partial* model is used complicates severally the establishment of LSPs.

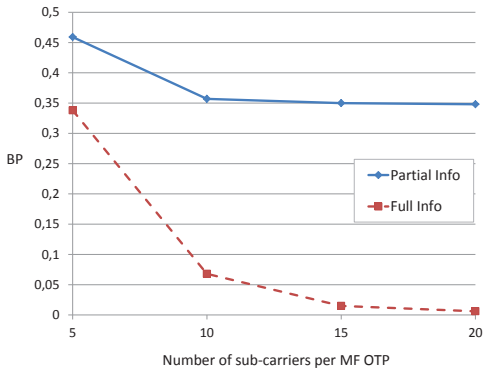

Fig. 7. BP vs. number of sub-carriers per MF-OTP for *partial* and *full* models.

VI. CONCLUSIONS

MF-OTPs are considered as key elements to improve the flexibility and reconfigurability within EONs. Indeed, MF-OTPs lead the support of different data client rates (including super-channels connections) attaining an efficient use of the overall network optical spectrum. In this context, we devise an on-line distance-adaptive RSMA algorithm (executed at the PCE) which dynamically serves flexgrid LSPs trying to optimize the use of both network optical spectrum (from an end-to-end perspective) as well as MF-OTP resources (i.e., sub-carriers). Required routing and signaling extensions have been designed and experimentally validated. These protocol extensions enable to automatically discover, select and configure the MF-OTP resources at the LSP endpoints. For the routing protocol (OSPF-TE) extensions, two information models are proposed: *partial* and *full*. For the signaling protocol (RSVP-TE), an explicit transponder control extends the ERO specifying the set of sub-carriers and their attributes (e.g., FS, modulation format, etc.) to accommodate flexgrid LSPs. Besides validating those protocol extensions, the experimental evaluation of the proposed RSMA algorithm adopting both information models is conducted in the ADRENALINE testbed. In light of the results, we conclude that the use of *full* model does attain a better performance in terms of the connection blocking compared to the *partial* strategy. This enhancement is, however, achieved at the expenses of increasing the control overhead since more MF-OTP capabilities and attributes need to be flooded within the *full* model.

ACKNOWLEDGMENTS

Work funded partially by the Spanish MINECO project FARO (TEC2012-38119) and EU FP7 project IDEALIST (317999).

REFERENCES

[1] N. Sambo, et. al., "Next Generation Sliceable Bandwidth Variable Transponders," *IEEE Comm. Mag.*, vol. 53, no. 2, February 2015.
[2] M. Jinno, et. al., "Spectrum-Efficient and Scalable Elastic Optical Path Network: Archtitecture, Benefits, and Enabling Technologies," *IEEE Commun. Mag.*, vol. 47, no. 11, November 2009.
[3] ITU-T Recommendation G.694.1, "Spectral grids for wdm applications: Dwdm frequency grid," 2012.
[4] O. Gonzalez de Dios and R. Casellas, "Framework and Requirements for GMPLS-based control of Flex-grid DWDM networks," *IETF draft-ietf-ccamp-flexi-grid-fwk-03 (work in progress)*, February 2015.
[5] Y. Sone, et. al., "Bandwidth Squeezed Restoration in Spectrum-Sliced Elastic Optical Path Networks (SLICE)," *IEEE/OSA J. Opt. Commun. Netw.*, vol. 3, no. 3, March 2011.
[6] M. Jinno, et. al., "Distance-Adaptive Spectrum Resource Allocation in Spectrum-Sliced Elastic Optical Path Network," *IEEE Commun. Mag.*, vol. 48, no. 8, August 2010.
[7] M. Jinno, H. Takara, Y. Sone, K. Yonenaga, and A. Hirano, "Multiflow Optical Transponder for Efficient Multilayer Optical Networking," *IEEE Commun. Mag.*, vol. 50, no. 5, May 2012.
[8] R. Martinez, R. Casellas, R. Vilalta, and R. Muñoz, "Experimental Assessment of GMPLS/PCE-controlled Multi-Flow Optical Transponders in Flexgrid Networks," in *in Proc. of Optical Fiber Communication Conference and Exposition (OFC)*, Los Angeles, California, USA, March 2015.
[9] R. Casellas, et. al., "Design and Experimental Validation of a GMPLS/PCE Control Plane for Elastic CO-OFDM Optical Networks," *IEEE J. on Selected Areas in Commun.*, vol. 31, no. 1, January 2013.

[10] F. Cugini, et. al., "Demonstration of Flexible Optical Network Based on Path Computation Element," *IEEE J. Lightw. Technol.*, vol. 30, no. 5, March 2012.
[11] N. Sambo, et. al., "Sliceable Transponder Architecture Including Multiwavelength Source," *IEEE/OSA J. Opt. Commun. Netw.*, vol. 6, no. 7, July 2014.
[12] R. Casellas, R. Muñoz, J. M. Fabrega, M. S. Moreolo, R. Martinez, L. Liu, T. Tsuritani, and I. Morita, "Design and experimental validation of a gmpls/pce control plane for elastic co-ofdm optical networks," *IEEE Journal of Selected Areas in Communications (JSAC), special issue on Next-Generation Spectrum-Efficient and Elastic Optical Transport Networks*, vol. 31, no. 1, pp. 49–61, January 2013.
[13] Nicola Sambo et. al., "First demonstration of SDN-controlled SBVT based on multi-wavelength source with programmable and asymmetric channel spacing," in *in Proc. of European Conference on Optical Communications (ECOC)*, Cannes, France, Sept. 2014.
[14] R. Muñoz, R. Casellas, R. Vilalta, and R. Martinez, "Dynamic and Adaptive Control Plane Solutions for Flexi-Grid Optical Networks Based on Stateful PCE," *IEEE J. Lightw. Technol.*, vol. 32, no. 16, August 2014.
[15] K. Kompella and Y. Rehkter, "OSPF Extensions in Support of Generalized Multi-Protocol Label Switching (GMPLS)," *IETF RFC 4203*, October 2005.
[16] X. Zhang, H. Zheng, R. Casellas, O. Gonzales de Dios, and D. Ceccarelli, "GMPLS OSPF-TE Extensions in Support of Flexible Grid," *IETF draft-ietf-ccamp-flexible-ospf-ext-01 (work in progress)*, December 2014.
[17] G. Bernstein, Y. Lee, D. Li, and W. Imajuku, " General Network Element Constraint Encoding for GMPLS Controlled Networks," *IETF draft-ietf-ccamp-general-constraint-encode-20 (work in progress)*, February 2015.
[18] L. Velasco, A. Castro, M. Ruiz, and G. Junyent, "Solving Routing and Spectrum Allocation Related Optimization Problems: From Off-Line to In-Operation Flexgrid Network Planning," *IEEE J. Lightw. Technol.*, vol. 32, no. 16, August 2014.
[19] R. Munoz, R. Martinez, and R. Casellas, "Challenges for GMPLS lightpath provisioning in transparent optical networks: wavelength constraints in routing and signaling," *IEEE Commun. Mag.*, vol. 47, no. 8, August 2009.

Ricardo Martínez (SM'14) graduated and PhD in telecommunications engineering by the UPC-BarcelonaTech university in 2002 and 2007, respectively. He has been actively involved in several public-funded (national and EU) R&D as well as industrial technology transfer projects. Since 2013, he is Senior Researcher of the Communication Networks Division (CND) at CTTC. His research interests include control and network management architectures, protocols and traffic engineering mechanisms for next-generation packet and optical transport networks within aggregation/metro and core segments.

Ramon Casellas (SM'12) graduated in telecommunications engineering in 1999 by both the UPC-BarcelonaTech university and ENST Telecom Paristech, within an Erasmus/Socrates double degree program. After working as an undergraduate researcher at both France Telecom R&D and British Telecom Labs, he completed a Ph.D. degree in 2002. He worked as an associate professor at the networks and computer science department of the ENST (Paris) and joined the CTTC Optical Networking Area in 2006, with a Torres Quevedo research grant.

He currently is a senior research associate and the coordinator of the ADRENALINE testbed. He has been involved in several international R&D and technology transfer projects. His research interests include network control and management, the GMPLS/PCE architecture and protocols, software defined networking and traffic engineering mechanisms. He contributes to IETF standardization within the CCAMP and PCE working groups. He is a member of the IEEE Communications Society and a member of the Internet Society.

Ricard Vilalta graduated in telecommunications engineering in 2007 and received a Ph.D. degree in telecommunications in 2013, both from the Universitat Politècnica de Catalunya (UPC), Spain. He also has studied Audiovisual Communication at UOC (Open University of Catalonia) and is a master degree on Technology-based business innovation and administration at Barcelona University (UB). Since 2010, Ricard Vilalta is a researcher at CTTC, in the Optical Networks and Systems Department. His research is focussed on Optical Network Virtualization and Optical Openflow. He is currently a Research Associate at Open Networking Foundation.

Raül Muñoz (SM'12) graduated in telecommunications engineering in 2001 and received a Ph.D. degree in telecommunications in 2005, both from the Universitat Politècnica de Catalunya (UPC), Spain. After working as undergraduate researcher at Telecom Italia Lab (Turin, Italy) in 2000, and as assistant professor at the UPC in 2001, he joined the Centre Tecnològic de Telecomunicacions de Catalunya (CTTC) in 2002.

Currently, he is Senior Researcher, Head of the Optical Network and System Department, and Manager of the Communication Networks Division. Since 2000, he has participated in several R&D projects funded by the European Commission's Framework Programmes (FP7 FP6 and FP5) and the Spanish Ministries, as well as technology transfer projects. He has led several Spanish research projects, and currently leads the European Consortium of the EU-Japan project STRAUSS. His research interests include control and management architectures, protocols and traffic engineering algorithms for future optical transport networks.